Published in final edited form as:

Metabolism. 2019 April ; 93: 1–9. doi:10.1016/j.metabol.2018.12.003.

Ectopic lipid deposition mediates insulin resistance in adipose specific 11β-Hydroxysteroid Dehydrogenase type 1 transgenic mice

Abudukadier Abulizi[a], **João-Paulo Camporez**[a,1], **Dongyan Zhang**[a], **Varman T. Samuel**[a,c], **Gerald I. Shulman**[a,b], and **Daniel F. Vatner**[a]

[a]Department of Internal Medicine, Yale University School of Medicine, New Haven CT,06520, USA

[b]Department of Cellular & Molecular Physiology, Yale University School of Medicine, New Haven CT, 06520, USA

[c]Veterans Affairs Medical Center, West Haven CT, 06516, USA

Abstract

Context: Excessive adipose glucocorticoid action is associated with insulin resistance, but the mechanisms linking adipose glucocorticoid action to insulin resistance are still debated. We hypothesized that insulin resistance from excess glucocorticoid action may be attributed in part to increased ectopic lipid deposition in liver.

Methods: We tested this hypothesis in the adipose specific 11β-Hydroxysteroid dehydrogenase-1 (HSD11B1) transgenic mouse, an established model of adipose glucocorticoid excess. Tissue specific insulin action was assessed by hyperinsulinemic-euglycemic clamps, hepatic lipid content was measured, hepatic insulin signaling was assessed by immunoblotting. The role of hepatic lipid content was further probed by administration of the functionally liver-targeted mitochondrial uncoupler, Controlled Release Mitochondrial Protonophore (CRMP).

Findings: High fat diet fed HSD11B1 transgenic mice developed more severe hepatic insulin resistance than littermate controls (endogenous suppression of hepatic glucose production was reduced by 3.8-fold, $P < 0.05$); this was reflected by decreased insulin-stimulated hepatic insulin receptor kinase tyrosine phosphorylation and AKT serine phosphorylation. Hepatic insulin

Address for Correspondence: Daniel F. Vatner M.D. Ph.D., daniel.vatner@yale.edu, PO Box 208020, New Haven, CT 06520.

9.CONTRIBUTORS

A.A. performed and supervised experiments, analyzed data, and wrote and edited the manuscript. J.C. performed and supervised experiments, analyzed data, and edited the manuscript. D.Z. performed experiments. V.T.S. and G.I.S. conceived the study, supervised the study, and edited the manuscript. D.F.V. conceived the study, performed experiments, analyzed data, supervised the study, wrote and edited the manuscript. All authors reviewed the manuscript critically for intellectual content, and all authors approved the final version.

[1]Present Address: Department of Physiology and Biophysics, Institute of Biomedical Sciences, University of Sao Paulo, Sao Paulo/SP - CEP: 05508-000, Brazil.

8.COMPETING INTERESTS

Declarations of interest: None.

resistance was associated with a 53% increase ($P < 0.05$) in hepatic triglyceride content, a 73% increase in diacylglycerol content ($P < 0.01$), and a 66% increase in PKCε translocation ($P < 0.05$). Hepatic insulin resistance was prevented with administration of CRMP by reversal of hepatic steatosis and prevention of hepatic diacylglycerol accumulation and PKCε activation.

Conclusions: These findings are consistent with excess adipose glucocorticoid activity being a predisposing factor for the development of lipid (diacylglycerol-PKCε)-induced hepatic insulin resistance.

Keywords

Glucocorticoids; insulin resistance; nonalcoholic fatty liver disease; white adipose tissue

1. INTRODUCTION

Disordered adipose glucocorticoid metabolism has been implicated in the pathogenesis of insulin resistance and type 2 diabetes (T2D). Specifically, increased adipose 11β-hydroxysteroid dehydrogenase type 1 (HSD11B1) activity, which regenerates active cortisol from inactive metabolites, has been associated with obesity and insulin resistance in humans [1, 2] with obesity and insulin resistance; furthermore, a mouse model with adipose specific overexpression of HSD11B1 [3, 4] readily develops obesity and insulin resistance. In contrast, whole-body HSD11B1 knockout [5] and HSD11B2 overexpression (which inactivates corticosterone and cortisol) in adipose [6] both protect from obesity and insulin resistance. Knockdown of HSD11B1 in adipose tissue with shRNA prevents high-dose glucocorticoid induced glucose intolerance in mice [7]. Additionally, pharmacologic knockdown of the glucocorticoid receptor in adipose and liver with an antisense oligonucleotide led to reductions in plasma glucose, insulin, and basal glucose production in multiple rodent models [8]. However, thus far studies of adipose-specific glucocorticoid receptor knockout mice have produced conflicting results. One study demonstrated attenuated weight gain, adiposity, hepatic steatosis, and glucose intolerance [9], while another demonstrated no protection from hepatic steatosis and exacerbation of high fat diet induced glucose intolerance [10].

These disparate results highlight the lack of a clear mechanisms linking adipose glucocorticoid action to insulin resistance. Prevailing hypotheses for the relationship between increased adipose glucocorticoid metabolism and insulin resistance have proposed that increased release of regenerated cortisol from specific adipose beds (e.g. visceral adipose tissue) alter hepatic glucose and lipid metabolism, or that increased adipose glucocorticoid action alters local immune infiltrates and/or circulating adipokine profiles [3, 11]. In this work we sought to test an alternative hypothesis: that altered adipose glucocorticoid action drives alterations in adipose function resulting in increased ectopic lipid deposition and lipid-induced insulin resistance.

The link between increased adipose glucocorticoid action and ectopic lipid deposition is supported by several studies. In humans, single nucleotide polymorphisms in the HSD11B1 gene are associated with changes in hepatic fat deposition [12]. Whole-body pharmacologic HSD11B1 inhibition in mice reduces hepatic steatosis, though this has been attributed to

potentially increased hepatic lipid oxidation [13]. In contrast, liver-specific HSD11B1 knockout mice [14] were not significantly protected from the development of hepatic steatosis or dysregulated glucose metabolism when fed a high fat diet. We propose that changes in hepatic steatosis seen with whole body HSD11B1 knockdown may be attributed in large part to changes in glucocorticoid action in white adipose tissue (WAT), and these changes in ectopic lipid drive alterations in insulin action.

To examine this hypothesis, we placed HSD11B1 Tg mice on a high fat diet (HFD) and assessed *in vivo* tissue specific insulin action by the hyperinsulinemic-euglycemic clamp technique. Since body weight can be a confounding factor in metabolic studies, and HSD11B1 Tg mice gain more weight than wild type mice as they get older, we studied these mice before body weights diverged. We also sought to establish whether hepatic lipid accumulation was necessary for the development of hepatic insulin resistance. We used a mitochondrial protonophore which specifically increases hepatic lipid oxidation and prevents fatty liver, and assessed insulin sensitivity in HFD fed HSD11B1 Tg mice. Thus, these studies test whether ectopic lipid accumulation provides a link between excess adipose glucocorticoid action and impaired hepatic insulin action.

2. METHODS

2.1 Animals

Adipose specific HSD11B1 transgenic mice (transgene under the aP2 promoter) on an FVB/NTac background were obtained from Charles River Laboratory and were bred with wild type FVB/NTac mice obtained from Taconic. Studies were performed in age-matched mice (8-12 weeks old), transgenic mice were studied against littermate controls. Rodents were housed in accordance with the Guide for the care and use of laboratory animals and standard operating procedures of the Yale Animal Resource Center. Mice were multiply housed (2-5/standard cage, when possible) at 72±2° F, 30-70% humidity, with a 12:12 hr light/dark cycle, in individually vented cage racks on corncob bedding. Chlorinated water was provided either by automatic water or bottles. Male mice were chosen for all studies. For hyperinsulinemic clamp studies, jugular vein catheters were placed. At least six days were allowed for recovery from surgery before infusions were performed. Rodents were maintained on standard regular chow (Envigo 2108S: 24% protein/ 58% carbohydrate/ 18% fat calories); high fat feeding was performed with a standard high fat diet (Research Diets D12492: 20% protein/ 20% carbohydrate/ 60% fat calories) or a matched high fat diet containing 7.5 g continuous release mitochondrial protonophore (CRMP) per kg diet. Mice were allocated to experimental group by genotype; in experiments in which CRMP was used, assignment to HFD or HFD + CRMP was performed in a randomized fashion. Basal tissues were taken under isoflurane anesthesia in the early afternoon after a 6 hour fast and infusions were performed in the awake state in the morning following an overnight fast.

All procedures were approved by the Institutional Animal Care and Use Committee of the Yale University School of Medicine. This study was carried out in strict accordance with the recommendations in the Guide for the Care and Use of Laboratory Animals of the National Institutes of Health. Surgeries were performed under isoflurane anesthesia, and carprofen analgesia was provided in the postoperative period. All euthanasia was performed either

with intravenous pentobarbital in animals with jugular vein catheters, or under isoflurane anesthesia in non-catheterized animals. Care was taken throughout the study to minimize suffering.

2.2 Plasma Biochemical Analysis

Glucose concentrations were determined using a YSI (2700 select) or with a standard kit (Sekisui). Standard kits were also used to measure plasma fatty acids (Wako) and triglycerides (Sekisui). Insulin concentrations were determined by radioimmunoassay (EMD Millipore). Leptin concentrations were determined by ELISA (Abcam). Plasma m+16 palmitate enrichment was assessed by GC/MS after extraction from 5-10 μL plasma in chloroform:methanol as previously described [15].

2.3 Hyperinsulinemic-euglycemic clamp studies

Hyperinsulinemic-euglycemic clamps were performed as previously described [16]. [3-^{3}H]glucose (Perkin-Elmer) was infused at a rate of 0.05 μCi/min for 120 min to assess basal turnover. Following the basal infusion, human insulin (Novo Nordisk) was given as a prime [7.14 mU/(kg-min) ×3 min] then continuous [2.5 mU/(kg-min)] infusion; along with a variable infusion of 20% dextrose to maintain euglycemia (100-120 mg/dL), and [3-^{3}H]glucose at a rate of 0.1 μCi/min. During both basal and clamped periods, [$^{13}C_{16}$]palmitate was infused at 0.5-2.0 μmol/kg-min. Plasma samples were obtained by tail massage at 0, 25, 45, 65, 80, 90, 100, 110, 120, 130, and 140 min. At the end of the clamp, mice were anesthetized with pentobarbital, tissues were rapidly excised and snap-frozen in liquid nitrogen. In all conditions, turnover rates were determined by isotope dilution after the infusion reached steady state.

2.4 Tissue lipid isolation

Lipids were extracted from tissues in ice cold 2:1 chloroform:methanol. For triglyceride measurements, lipids were extracted with shaking at room temperature for 3-4 hours, and phase separation was achieved with H_2SO_4. For hepatic diacylglycerol measurements, lipids were first extracted from cytosolic/lipid droplet and membrane-associated fractions by a modified version of a previously described protocol [17]. Liver homogenates were separated by ultracentrifugation at 100,000xg for one hour. The pellet contains plasma membrane lipids while the supernatant contains cytosolic lipids, including lipid droplets. The chloroform:methanol extraction was then performed from each fraction, using water to achieve phase separation. The organic layer was removed, dried under nitrogen gas, and lipids were resuspended in hexane:methylene chloride:ether (89:10:1). Diacylglycerols were separated from triacylglycerols using a diol bonded SPE column (Waters) [18]. For hepatic ceramide measurements, choroform:methanol phase separation was achieved with water, and the organic layer was collected.

2.5 Tissue lipid measurements

Triglyceride content was measured using the Sekisui Triglyceride-SL kit (Sekisui). Diacylglycerols and ceramides were measured by LC-MS/MS as described previously [18], by a technician blinded to experimental group assignment.

2.6 Western blotting

Tissue was homogenized in ice-cold homogenization buffer with protease and phosphatase inhibitors (cOmplete MINI + PhosSTOP (Roche)). Proteins were resolved by SDS-PAGE using a 4-12% gradient gel and electroblotted onto polyvinylidene difluoride membrane (DuPont) using a semi-dry or wet-transfer cell. The membrane was then blocked with 5 % (w/v) nonfat dried milk or bovine serum albumin, and incubated overnight with primary antibody. After washing, membranes were incubated with horseradish peroxidase-conjugated secondary antibody (Cell Signaling Technology) for 60 minutes. Detection was performed with enhanced chemiluminescence.

For PKCε translocation, cytoplasm and plasma membrane were separated by ultracentrifugation as previously described [19, 20], and Western blotting was performed as described above.

Antibodies were purchased from: 1. Cell Signaling Technology- IRβ (3020S), phosphorylated IRβ (Tyr 1162, 3918S), Akt (2920S), phosphorylated Akt (Ser473, 9721S); BD Biosciences-PKCε (610086); Abcam Inc.- sodium potassium ATPase (Ab7671); Santa Cruz Biotechnology-GAPDH (sc-25778).

2.7 Body Composition and Metabolic Cage Studies

Body composition in mice was measured by ^{1}H magnetic resonance spectroscopy using a Bruker Minispec analyzer. Energy expenditure and caloric intake were measured in a Comprehensive Laboratory Animal Monitoring System (CLAMS; Columbus Instruments). Mice were allowed to acclimate to the metabolic cages for 24 hours before beginning data collection.

2.8 Oral fat tolerance tests

Overnight fasted mice received a gavage of vegetable oil (400 μL per mouse) labeled with ^{3}H triolein (Perkin Elmer, 10 μCi per mouse). Blood was sampled at 0,1,2,3,4, and 6 hours for total plasma triglyceride and for chylomicron measurement by scintillation counting.

2.9 Quantitative PCR

Total RNA was isolated from tissue using Qiazol (Qiagen) reagent and was further purified with the RNeasy kit (Qiagen). The abundance of transcripts was assessed by real-time PCR on an Applied Biosystems 7500 Fast Real-Time PCR System with a SYBR Green detection system (Bio-Rad). The expression data for each gene of interest were against β-actin as the invariant control and relative expression determined using amplification efficiencies [21]. Primer sequences: *β-actin F*- CCAGATCATGTTTGAGACCTTC; *R*-CATGAGGTAGTCTGTCAGGTCC; *Leptin* (From the PrimerBank Database: PrimerBank ID 34328437c1, https://pga.mgh.harvard.edu/primerbank/) *F*-GTGGCTTTGGTCCTATCTGTC; *R*-CGTGTGTGAAATGTCATTGATCC.

2.10 Statistical Analysis

Statistical analysis of the data, was performed using GraphPad Prism 7. When two groups were compared, the Student's unpaired T-test was used. When three or more groups were

compared, as all of the groups were mutually exclusive (i.e. transgenic mice treated with vehicle were not the same as the transgenic mice treated with CRMP), a one-way ANOVA analysis was used followed by Tukey's Multiple Comparison test. P values less than 0.05 were considered significant.

3. RESULTS

3.1 Basal parameters after two weeks high fat diet

Chronic high fat diet feeding leads to body weight divergence in adipose specific HSD11B1 transgenic (HSD Tg) mice after 3-4 weeks [3]. To avoid the confounding effect of obesity, we fed HSD Tg mice and littermate control mice (WT) high fat diet (HFD) for two weeks, with or without the Continuous Release Mitochondrial Protonophore (CRMP). Basal parameters were assessed after a six hour fast (Table 1). Body weight, epididymal adipose tissue weight, and plasma parameters were unaffected by genotype or CRMP treatment status.

3.2 High fat diet fed HSD Tg mice demonstrate reduced hepatic insulin sensitivity

We evaluated whole body and tissue specific insulin action after two weeks of high fat feeding using a hyperinsulinemic-euglycemic clamp. Euglycemia was maintained throughout the clamp period, and stable glucose infusion rates were achieved (Figure 1A-B). Hepatic insulin sensitivity, as assessed by insulin-mediated suppression of endogenous glucose production (EGP), was markedly reduced in HSD Tg mice as compared with WT; this phenotype was reversed by treatment with CRMP (Figure 1C-D). In contrast, whole body insulin mediated glucose disposal was unchanged with the adipose HSD11B1 transgene or with CRMP treatment (Figure 1E).

3.3 Lipid-induced hepatic insulin resistance is exacerbated by the adipose HSD11B1 transgene

The observed reversal of hepatic insulin resistance with CRMP treatment is consistent with lipotoxic hepatic insulin resistance. Hepatic triglyceride concentration was increased in HSD Tg mice (compared with WT), and this increase was prevented by CRMP treatment (Figure 2A). Similarly, whole cell DAG concentration, cytosolic fraction DAG concentration, and membrane fraction DAG concentration were all increased in HSD Tg mice, while these increases in DAG concentrations were prevented by treatment of HFD-fed HSD Tg mice with CRMP (Figure 2B-D, Supplemental Figure 1). Ceramides have also been implicated in the pathogenesis of lipid-induced insulin resistance. However, hepatic ceramide concentration was lower in the insulin resistant HSD Tg mice and not affected by CRMP treatment (Figure 2E).

Increases in hepatic *Sn*-1,2-DAG activate PKCε, which then impairs hepatocellular insulin signaling [22]. PKCε membrane translocation, a measure of PKCε activation, was increased in HSD Tg mice as compared with WT (Figure 3A). CRMP treatment normalized PKCε translocation. Activated PKCε can phosphorylate the insulin receptor kinase at threonine 1150, inhibiting its tyrosine kinase activity and downstream phosphorylation events [23]. Indeed, insulin mediated hepatic IRK auto-tyrosine phosphorylation was reduced by 46% in

HSD Tg mice as compared with WT, and was restored by CRMP treatment (Figure 3B). Similarly, insulin-stimulated Akt phosphorylation was reduced in HSD Tg mice, and was improved in HSD Tg mice treated with CRMP (Figure 3C).

3.4 Linking adipose glucocorticoid excess to ectopic lipid accumulation

White adipose tissue (WAT) dysfunction could cause ectopic lipid deposition by dysregulation of WAT lipolysis, alterations in whole-body energy balance, or impaired clearance of chylomicron triglyceride. WAT lipolysis was unchanged in HSD TG mice: neither plasma nonesterified fatty acid levels (Figure 4A) nor the rate of fatty acid flux in basal and hyperinsulinemic conditions (Figure 4B), was altered in HSD Tg mice. Energy balance was assessed in metabolic cages, monitoring energy expenditure by indirect calorimetry and energy intake by assessment of food consumption. HSD Tg mice had an increase in food intake (Figure 5A+C), while whole-mouse energy expenditure was unchanged (Figure 5B+D). Consistent with the observed increase in food intake, both fed-state plasma leptin concentration and WAT leptin mRNA expression were decreased in HSD Tg mice (Figure 5E+F). Oral fat tolerance tests were performed by gavage of vegetable oil labeled with ^{3}H triolein (Figure 6A) to assess postprandial plasma chylomicron clearance. Plasma chylomicron levels, as reflected by plasma ^{3}H, were higher in HSD Tg mice than WT mice (Figure 6B) and suggest impaired adipose clearance of chylomicron triglyceride. Thus, in the HSD Tg mouse, excess adipose glucocorticoid action may lead to hepatic steatosis by increasing net energy intake and reducing postprandial plasma triglyceride extraction.

4. DISCUSSION

Adipose glucocorticoid excess is associated with obesity and insulin resistance [3-8]; yet the underlying cellular mechanism causing this insulin resistance remains debated. Studies of the HSD Tg mouse, which recapitulates many features of the metabolic syndrome [3], did not clearly provide a mechanism accounting for insulin resistance. The numerous mechanisms that have been proposed largely focus on the release of some factor from the adipose tissue, such as glucocorticoids, cytokines or adipokines. The present studies offer an alternative mechanistic link between adipose glucocorticoid excess and hepatic insulin resistance. Specifically, adipose glucocorticoid excess leads to hepatic steatosis, *sn*-1,2-DAG mediated PKCε activation, and impaired insulin signaling. Treatment with a liver specific protonophore reverses the fatty liver, prevents PKCε activation and normalizes insulin signaling. Several aspects of this study merit further consideration, including how these studies differ from prior studies, what we can learn about how adipose glucocorticoid excess may cause ectopic lipid accumulation, and how this knowledge can inform drug development.

Our studies demonstrate that insulin resistance in HFD fed HSD Tg mice is largely attributed to ectopic lipid accumulation, without needing to invoke other adipose derived factors (e.g. adipokines, cytokines or excess glucocorticoid release). Short term fat fed HSD Tg mice were specifically prone to excess hepatic insulin resistance, while peripheral insulin action as reflected by glucose disposal during the clamp was unaffected by the adipose

transgene. The ability of CRMP, at doses where it is a liver-specific mitochondrial uncoupler [24] with little accumulation in extrahepatic tissues, to reverse hepatic insulin resistance in HSD Tg mice further supports the hypothesis that it is the ectopic lipid accumulation that causes insulin resistance in this model. In addition, in all three models (WT, HSD Tg and HSD Tg+CRMP) hepatic DAG content was concordant with PKCε activation and with hepatic insulin resistance. In contrast, there was no relation between hepatic ceramide content and insulin resistance. The observed discordance between hepatic diacylglycerol content and hepatic ceramide content may be somewhat surprising, but the biosynthesis of these lipids occurs by discrete pathways that may be regulated independent of one another.

The effect we observed of CRMP on HSD Tg mice mimics the effects of CRMP (and the mechanistically related uncoupler, DNP-ME) on HFD-fed wild type rodents and on lipodystrophic regular chow fed mice, as we observed reduced hepatic lipid content and improved hepatic insulin sensitivity [24-26]. Of note, the prior studies of functionally liver targeted mitochondrial uncouplers demonstrated no effect of these uncouplers on either whole animal energy expenditure or on food intake; these uncouplers specifically exert their metabolic effects by depletion of hepatic lipid content.

The present studies had several key differences from prior studies of HSD Tg mice. Previous studies of HSD Tg mice were done after a divergence in body weight (high fat diet fed HSD Tg mice diverge in body weight with respect to wild type mice in early adulthood) [3]. This marked weight difference would introduce multiple confounding factors. Chronic obesity alters whole body metabolism in many ways, such as by increased inflammation or alterations in mitochondrial content [27, 28], while hepatic insulin resistance is an early finding in HSD Tg mice specifically associated with ectopic lipid.

HSD Tg mice have two key changes that lead to ectopic lipid accumulation: they have increased food intake and decreased postprandial plasma lipid clearance. Appetite dysregulation is an important mechanism by which adipose glucocorticoid excess could lead to ectopic lipid deposition in weight-matched HSD Tg mice. A reduction in fed plasma leptin mRNA expression and plasma concentration is consistent with increased food intake. This finding was unexpected, as acute glucocorticoid exposure drives adipose leptin production, and previously HSD Tg mice were reported to be hyperleptinemic rather than hypoleptinemic [3]. Moreover, the reduction in adipose *Lep* expression was evident only in fed HSD Tg mice, not fasted. It may be that while acute glucocorticoid exposure drives leptin expression, chronic glucocorticoid action blunts physiological postprandial *Lep* expression. In addition, we report a reduction in postprandial triglyceride clearance in HSD Tg mice. This would divert more chylomicron remnants to the liver and fuel esterification of dietary fatty acids into hepatic lipid species. Finally, we did not observe increased lipolysis in the HSD Tg mice. The role of glucocorticoids in the regulation of lipolysis is complex: glucocorticoids can acutely promote adipose lipolysis [29], but excess circulating glucocorticoids may only be permissive for increased lipolysis in states where catecholamines or insulin are also altered [30]. In the HSD Tg mouse model, it may be that chronic increases in adipose glucocorticoid action lead to adaptive changes that dampen glucocorticoid mediated lipolysis. Nonetheless, altered adipose lipolysis does not appear to contribute to nonalcoholic fatty liver disease (NAFLD) and insulin resistance in this model.

Combining the effects of excess glucocorticoid action on adipose tissue described here with the known effects of glucocorticoids on hepatic lipid metabolism, we can assemble a more complete picture explaining how excess systemic glucocorticoids leads to NAFLD. Normal hepatic glucocorticoid action drives de novo lipogenesis and suppresses hepatic fatty acid oxidation [31]. Under routine, low-stress conditions, this glucocorticoid-driven lipid synthesis is likely balanced by glucocorticoid-stimulated VLDL secretion [31, 32]. In the setting of glucocorticoid excess this balance is disrupted, both by suppressed mobilization of stored intrahepatocellular triglyceride seen with excess hepatic glucocorticoid action [33], and by increased delivery of lipids to the liver due to excess adipose glucocorticoid action. To restore the balance of hepatic lipid metabolism in NAFLD, selective glucocorticoid receptor agonists have been developed, leveraging the beneficial effects of glucocorticoids on hepatic lipid metabolism while attempting to avoid the deleterious effects [34]. An improved understanding of excess adipose glucocorticoid action may help to inform further development of this intriguing pharmacologic strategy.

The role of adipose *HSD11B1* in human metabolic disease is incompletely understood. Evidence from studies of human physiology suggests there may be an interplay between whole body energy metabolism and subcutaneous WAT 11β-hydroxysteroid dehydrogenase activity. Circulating fatty acids and insulin appear to regulate WAT 11β-hydroxysteroid dehydrogenase-1 activity in lean but not obese patients [35, 36]. Studies of the *HSD11B1* gene are conflicted regarding a relationship with metabolic disease. Polymorphisms in the *HSD11B1* gene are associated with fatty liver and type 2 diabetes (T2D) with or without metabolic syndrome [12, 37, 38]. Adipose *HSD11B1* expression and activity are sometimes seen to correlate with insulin resistance or polycystic ovary syndrome [39-43]; while other studies show *HSD11B1* expression correlates with obesity rather than metabolic disease [38, 44], and the relationship between gene expression and fasting insulin may vary depending on tissue bed [45]. Such conflicting data underscores the need for both mechanistic and clinical investigations of the effects of adipose tissue glucocorticoid action.

Certainly, adipose glucocorticoid excess may be an aspect of adipose dysfunction that drives metabolic derangements in obese humans. As such, addressing the question of how adipose glucocorticoid action modulates systemic insulin action is not simply an academic exercise, rather it could impact our understanding of the pathophysiology of insulin resistance and inform therapeutic strategies. The results of this study of HSD Tg mice may help to explain the mixed results seen in phase 2 trials of inhibitors of 11β-hydroxysteroid dehydrogenase for the treatment of Type 2 Diabetes [46, 47]. If the metabolic consequences of excess adipose glucocorticoid action are due to ectopic lipid accumulation, then the efficacy of alteration of glucocorticoid activation pathways may be blunted without concomitant reversal of ectopic lipid accumulation.

5. CONCLUSIONS

In summary, adipose glucocorticoid excess in mice exacerbates hepatic insulin resistance through the development of hepatic steatosis and DAG-nPKC mediated lipotoxicity. Increased adipose *HSD11B1* expression may predispose patients to metabolic disease by the same mechanisms. Treatments directed at amelioration of ectopic fat deposition, either by

redirection of fat to eutopic white adipose tissue storage or by increasing fat catabolism, will be central to any such insulin sensitizing strategy.

Supplementary Material

Refer to Web version on PubMed Central for supplementary material.

ACKNOWLEDGEMENTS

We would like to thank Mario Kahn, Gina Butrico, Ali Nasiri, Xiaoxian Ma, Codruta Todeasa, and Maria Batsu, and the Yale Diabetes Research Core facility (Yale University School of Medicine) for excellent technical support.

7. FUNDING SOURCES

This work was supported by the National Institutes of Health (K23 DK-10287, R01 DK-113984, P30 DK-045735); and the Veterans Health Administration (Merit Review Award I01 BX000901).

Abbreviations

HSD11B1	11β-Hydroxysteroid dehydrogenase-1
CRMP	Controlled Release Mitochondrial Protonophore
AKT	Protein kinase B
PKC	Protein kinase C
nPKC	Novel protein kinase C
T2D	Type 2 diabetes
HSD Tg	Adipose HSD11B1 transgenic
WT	Wild type
IRβ/IRK	Insulin receptor β/Insulin receptor kinase
GAPDH	Glyceraldehyde 3-phosphate dehydrogenase
LC-MS/MS	Liquid chromatography with tandem mass spectrometry
EGP	Endogenous glucose production
DAG	Diacylglycerol
WAT	White adipose tissue
DNP-ME	Dinitrophenol-methyl ester

REFERENCES

[1]. Bujalska IJ, Kumar S, Stewart PM. Does central obesity reflect "Cushing's disease of the omentum"? Lancet. 1997;349:1210–3. [PubMed: 9130942]

[2]. Rask E, Olsson T, Soderberg S, Andrew R, Livingstone DE, Johnson O, et al. Tissue-specific dysregulation of cortisol metabolism in human obesity. The Journal of clinical endocrinology and metabolism. 2001;86:1418–21. [PubMed: 11238541]

[3]. Masuzaki H, Paterson J, Shinyama H, Morton NM, Mullins JJ, Seckl JR, et al. A transgenic model of visceral obesity and the metabolic syndrome. Science. 2001;294:2166–70. [PubMed: 11739957]

[4]. Masuzaki H, Yamamoto H, Kenyon CJ, Elmquist JK, Morton NM, Paterson JM, et al. Transgenic amplification of glucocorticoid action in adipose tissue causes high blood pressure in mice. The Journal of clinical investigation. 2003;112:83–90. [PubMed: 12840062]

[5]. Morton NM, Paterson JM, Masuzaki H, Holmes MC, Staels B, Fievet C, et al. Novel adipose tissue-mediated resistance to diet-induced visceral obesity in 11 beta-hydroxysteroid dehydrogenase type 1-deficient mice. Diabetes. 2004;53:931–8. [PubMed: 15047607]

[6]. Kershaw EE, Morton NM, Dhillon H, Ramage L, Seckl JR, Flier JS. Adipocyte-specific glucocorticoid inactivation protects against diet-induced obesity. Diabetes. 2005;54:1023–31. [PubMed: 15793240]

[7]. Wang Y, Yan C, Liu L, Wang W, Du H, Fan W, et al. 11beta-Hydroxysteroid dehydrogenase type 1 shRNA ameliorates glucocorticoid-induced insulin resistance and lipolysis in mouse abdominal adipose tissue. American journal of physiology Endocrinology and metabolism. 2015;308:E84–95. [PubMed: 25389364]

[8]. Watts LM, Manchem VP, Leedom TA, Rivard AL, McKay RA, Bao D, et al. Reduction of hepatic and adipose tissue glucocorticoid receptor expression with antisense oligonucleotides improves hyperglycemia and hyperlipidemia in diabetic rodents without causing systemic glucocorticoid antagonism. Diabetes. 2005;54:1846–53. [PubMed: 15919808]

[9]. Mueller KM, Hartmann K, Kaltenecker D, Vettorazzi S, Bauer M, Mauser L, et al. Adipocyte Glucocorticoid Receptor Deficiency Attenuates Aging- and HFD-Induced Obesity and Impairs the Feeding-Fasting Transition. Diabetes. 2017;66:272–86. [PubMed: 27650854]

[10]. Desarzens S, Faresse N. Adipocyte glucocorticoid receptor has a minor contribution in adipose tissue growth. The Journal of endocrinology. 2016;230:1–11. [PubMed: 27106108]

[11]. Pereira CD, Azevedo I, Monteiro R, Martins MJ. 11beta-Hydroxysteroid dehydrogenase type 1: relevance of its modulation in the pathophysiology of obesity, the metabolic syndrome and type 2 diabetes mellitus. Diabetes, obesity & metabolism. 2012;14:869–81.

[12]. Lutz SZ, Peter A, Machicao F, Lamprinou A, Machann J, Schick F, et al. Genetic Variation in the 11beta-hydroxysteroid-dehydrogenase 1 Gene Determines NAFLD and Visceral Obesity. The Journal of clinical endocrinology and metabolism. 2016;101:4743–51. [PubMed: 27715400]

[13]. Berthiaume M, Laplante M, Festuccia WT, Berger JP, Thieringer R, Deshaies Y. Preliminary report: pharmacologic 11beta-hydroxysteroid dehydrogenase type 1 inhibition increases hepatic fat oxidation in vivo and expression of related genes in rats fed an obesogenic diet. Metabolism: clinical and experimental. 2010;59:114–7. [PubMed: 19766266]

[14]. Lavery GG, Zielinska AE, Gathercole LL, Hughes B, Semjonous N, Guest P, et al. Lack of significant metabolic abnormalities in mice with liver-specific disruption of 11beta-hydroxysteroid dehydrogenase type 1. Endocrinology. 2012;153:3236–48. [PubMed: 22555437]

[15]. Perry RJ, Peng L, Abulizi A, Kennedy L, Cline GW, Shulman GI. Mechanism for leptin's acute insulin-independent effect to reverse diabetic ketoacidosis. The Journal of clinical investigation. 2017;127:657–69. [PubMed: 28112679]

[16]. Camporez JP, Jornayvaz FR, Lee HY, Kanda S, Guigni BA, Kahn M, et al. Cellular mechanism by which estradiol protects female ovariectomized mice from high-fat diet-induced hepatic and muscle insulin resistance. Endocrinology. 2013;154:1021–8. [PubMed: 23364948]

[17]. Bogan JS, McKee AE, Lodish HF. Insulin-responsive compartments containing GLUT4 in 3T3-L1 and CHO cells: regulation by amino acid concentrations. Molecular and cellular biology. 2001;21:4785–806. [PubMed: 11416153]

[18]. Yu C, Chen Y, Cline GW, Zhang D, Zong H, Wang Y, et al. Mechanism by which fatty acids inhibit insulin activation of insulin receptor substrate-1 (IRS-1)-associated phosphatidylinositol 3-kinase activity in muscle. The Journal of biological chemistry. 2002;277:50230–6. [PubMed: 12006582]

[19]. Kumashiro N, Erion DM, Zhang D, Kahn M, Beddow SA, Chu X, et al. Cellular mechanism of insulin resistance in nonalcoholic fatty liver disease. Proc Natl Acad Sci U S A. 2011;108:16381–5. [PubMed: 21930939]

[20]. Qu X, Seale JP, Donnelly R. Tissue and isoform-selective activation of protein kinase C in insulin-resistant obese Zucker rats - effects of feeding. The Journal of endocrinology. 1999;162:207–14. [PubMed: 10425458]

[21]. Pfaffl MW. A new mathematical model for relative quantification in real-time RT-PCR. Nucleic acids research. 2001;29:e45. [PubMed: 11328886]

[22]. Samuel VT, Shulman GI. The pathogenesis of insulin resistance: integrating signaling pathways and substrate flux. J Clin Invest. 2016;126:12–22. [PubMed: 26727229]

[23]. Petersen MC, Madiraju AK, Gassaway BM, Marcel M, Nasiri AR, Butrico G, et al. Insulin receptor Thr1160 phosphorylation mediates lipid-induced hepatic insulin resistance. The Journal of clinical investigation. 2016.

[24]. Perry RJ, Zhang D, Zhang XM, Boyer JL, Shulman GI. Controlled-release mitochondrial protonophore reverses diabetes and steatohepatitis in rats. Science. 2015;347:1253–6. [PubMed: 25721504]

[25]. Perry RJ, Kim T, Zhang XM, Lee HY, Pesta D, Popov VB, et al. Reversal of hypertriglyceridemia, fatty liver disease, and insulin resistance by a liver-targeted mitochondrial uncoupler. Cell metabolism. 2013;18:740–8. [PubMed: 24206666]

[26]. Abulizi A, Perry RJ, Camporez JPG, Jurczak MJ, Petersen KF, Aspichueta P, et al. A controlled-release mitochondrial protonophore reverses hypertriglyceridemia, nonalcoholic steatohepatitis, and diabetes in lipodystrophic mice. FASEB journal : official publication of the Federation of American Societies for Experimental Biology. 2017;31:2916–24. [PubMed: 28330852]

[27]. Lee YS, Li P, Huh JY, Hwang IJ, Lu M, Kim JI, et al. Inflammation is necessary for long-term but not short-term high-fat diet-induced insulin resistance. Diabetes. 2011;60:2474–83. [PubMed: 21911747]

[28]. Sutherland LN, Capozzi LC, Turchinsky NJ, Bell RC, Wright DC. Time course of high-fat diet-induced reductions in adipose tissue mitochondrial proteins: potential mechanisms and the relationship to glucose intolerance. American journal of physiology Endocrinology and metabolism. 2008;295:E1076–83. [PubMed: 18780775]

[29]. Wang JC, Gray NE, Kuo T, Harris CA. Regulation of triglyceride metabolism by glucocorticoid receptor. Cell Biosci. 2012;2:19. [PubMed: 22640645]

[30]. Stimson RH, Anderson AJ, Ramage LE, Macfarlane DP, de Beaux AC, Mole DJ, et al. Acute physiological effects of glucocorticoids on fuel metabolism in humans are permissive but not direct. Diabetes, obesity & metabolism. 2017;19:883–91.

[31]. Li G, Hernandez-Ono A, Crooke RM, Graham MJ, Ginsberg HN. Effects of antisense-mediated inhibition of 11beta-hydroxysteroid dehydrogenase type 1 on hepatic lipid metabolism. Journal of lipid research. 2011;52:971–81. [PubMed: 21364201]

[32]. Berthiaume M, Laplante M, Festuccia WT, Cianflone K, Turcotte LP, Joanisse DR, et al. 11beta-HSD1 inhibition improves triglyceridemia through reduced liver VLDL secretion and partitions lipids toward oxidative tissues. American journal of physiology Endocrinology and metabolism. 2007;293:E1045–52. [PubMed: 17666487]

[33]. Dolinsky VW, Douglas DN, Lehner R, Vance DE. Regulation of the enzymes of hepatic microsomal triacylglycerol lipolysis and re-esterification by the glucocorticoid dexamethasone. The Biochemical journal. 2004;378:967–74. [PubMed: 14662008]

[34]. Koorneef LL, van den Heuvel JK, Kroon J, Boon MR, t Hoen PAC, Hettne KM, et al. Selective Glucocorticoid Receptor Modulation Prevents and Reverses Nonalcoholic Fatty Liver Disease in Male Mice. Endocrinology. 2018;159:3925–36. [PubMed: 30321321]

[35]. Wake DJ, Homer NZ, Andrew R, Walker BR. Acute in vivo regulation of 11beta-hydroxysteroid dehydrogenase type 1 activity by insulin and intralipid infusions in humans. The Journal of clinical endocrinology and metabolism. 2006;91:4682–8. [PubMed: 16954164]

[36]. Sandeep TC, Andrew R, Homer NZ, Andrews RC, Smith K, Walker BR. Increased in vivo regeneration of cortisol in adipose tissue in human obesity and effects of the 11beta-hydroxysteroid dehydrogenase type 1 inhibitor carbenoxolone. Diabetes. 2005;54:872–9. [PubMed: 15734867]

[37]. Devang N, Satyamoorthy K, Rai PS, Nandini M, Rao S, Phani NM, et al. Association of HSD11B1 gene polymorphisms with type 2 diabetes and metabolic syndrome in South Indian population. Diabetes Res Clin Pract. 2017;131:142–8. [PubMed: 28750217]

[38]. Nair S, Lee YH, Lindsay RS, Walker BR, Tataranni PA, Bogardus C, et al. 11beta-Hydroxysteroid dehydrogenase Type 1: genetic polymorphisms are associated with Type 2 diabetes in Pima Indians independently of obesity and expression in adipocyte and muscle. Diabetologia. 2004;47:1088–95. [PubMed: 15156315]

[39]. Svendsen PF, Madsbad S, Nilas L, Paulsen SK, Pedersen SB. Expression of 11beta-hydroxysteroid dehydrogenase 1 and 2 in subcutaneous adipose tissue of lean and obese women with and without polycystic ovary syndrome. Int J Obes (Lond). 2009;33:1249–56. [PubMed: 19704410]

[40]. Gambineri A, Fanelli F, Tomassoni F, Munarini A, Pagotto U, Andrew R, et al. Tissue-specific dysregulation of 11beta-hydroxysteroid dehydrogenase type 1 in overweight/obese women with polycystic ovary syndrome compared with weight-matched controls. Eur J Endocrinol. 2014;171:47–57. [PubMed: 24743397]

[41]. Koska J, de Courten B, Wake DJ, Nair S, Walker BR, Bunt JC, et al. 11beta-hydroxysteroid dehydrogenase type 1 in adipose tissue and prospective changes in body weight and insulin resistance. Obesity. 2006;14:1515–22. [PubMed: 17030962]

[42]. Lindsay RS, Wake DJ, Nair S, Bunt J, Livingstone DE, Permana PA, et al. Subcutaneous adipose 11 beta-hydroxysteroid dehydrogenase type 1 activity and messenger ribonucleic acid levels are associated with adiposity and insulinemia in Pima Indians and Caucasians. The Journal of clinical endocrinology and metabolism. 2003;88:2738–44. [PubMed: 12788882]

[43]. Baudrand R, Dominguez JM, Carvajal CA, Riquelme A, Campino C, Macchiavello S, et al. Overexpression of hepatic 5alpha-reductase and 11beta-hydroxysteroid dehydrogenase type 1 in visceral adipose tissue is associated with hyperinsulinemia in morbidly obese patients. Metabolism: clinical and experimental. 2011;60:1775–80. [PubMed: 21704348]

[44]. Gambineri A, Tomassoni F, Munarini A, Stimson RH, Mioni R, Pagotto U, et al. A combination of polymorphisms in HSD11B1 associates with in vivo 11{beta}-HSD1 activity and metabolic syndrome in women with and without polycystic ovary syndrome. Eur J Endocrinol. 2011;165:283–92. [PubMed: 21622477]

[45]. Baudrand R, Carvajal CA, Riquelme A, Morales M, Solis N, Pizarro M, et al. Overexpression of 11beta-hydroxysteroid dehydrogenase type 1 in hepatic and visceral adipose tissue is associated with metabolic disorders in morbidly obese patients. Obesity surgery. 2010;20:77–83. [PubMed: 19690925]

[46]. Feig PU, Shah S, Hermanowski-Vosatka A, Plotkin D, Springer MS, Donahue S, et al. Effects of an 11beta-hydroxysteroid dehydrogenase type 1 inhibitor, MK-0916, in patients with type 2 diabetes mellitus and metabolic syndrome. Diabetes, obesity & metabolism. 2011;13:498–504.

[47]. Rosenstock J, Banarer S, Fonseca VA, Inzucchi SE, Sun W, Yao W, et al. The 11-beta-hydroxysteroid dehydrogenase type 1 inhibitor INCB13739 improves hyperglycemia in patients with type 2 diabetes inadequately controlled by metformin monotherapy. Diabetes care. 2010;33:1516–22. [PubMed: 20413513]

Highlights

- Adipose glucocorticoid excess drives hepatic insulin resistance (IR) before obesity
- This IR is associated with hepatic steatosis; reversed by ectopic lipid depletion
- Hepatic IR is consistent with diacylglycerol-PKCε mediated IR
- More energy intake and reduced chylomicron clearance may explain hepatosteatosis

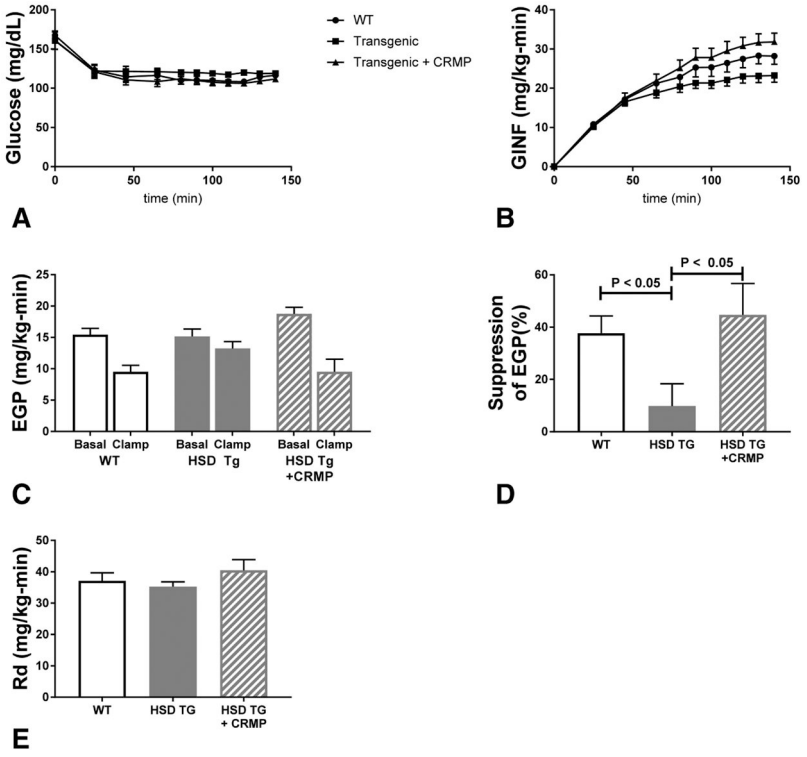

Figure 1. Hyperinsulinemic-euglycemic clamps.

Two week high fat diet fed Wild Type Fvb mice, HSD Tg mice, and HSD Tg mice treated with CRMP were studied by hyperinsulinemic euglycemic clamps. **A.** Plasma glucose during the clamp. **B.** Glucose infusion rate (GINF) during the clamp. **C.** Endogenous glucose production (EGP) in both the basal and hyperinsulinemic clamped state for each group. **D.** Insulin mediated suppression of EGP, represented as percent suppression. **E.** Insulin stimulated whole body glucose disposal (R_d). Insulin levels during the clamp were 83 ± 12 (WT), 67 ± 13 (HSD Tg), and 68 ± 8 (HSD Tg + CRMP)- insulin level differences were nonsignificant whether compared by ANOVA or students t-test. Data are the mean ± SEM of n = 11 (WT), n = 8 (HSD Tg), and n = 10 (HSD Tg + CRMP).

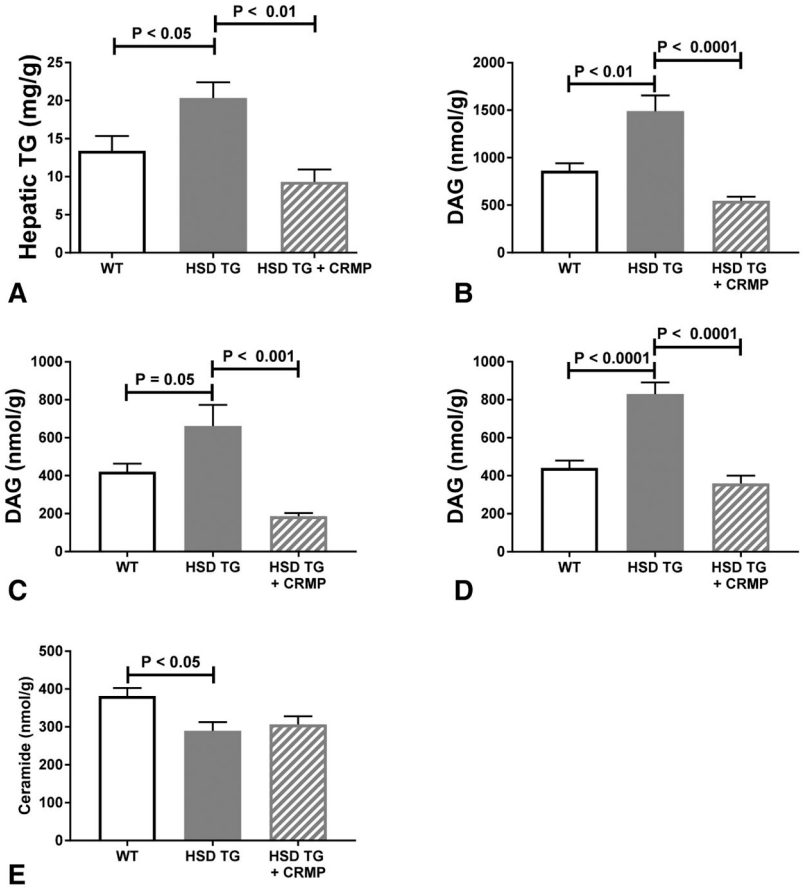

Figure 2. Hepatic lipid species.

Hepatic lipid species assessed in six hour fasted, two week high fat diet fed Wild Type Fvb mice, HSD Tg mice, and HSD Tg mice treated with CRMP. **A.** Hepatic triglyceride content. **B.** Hepatic total diacylglycerol (DAG) content. **C.** Hepatic cytoplasm + lipid droplet diacylglycerol content. **D.** Hepatic membrane diacylglycerol content. **E.** Hepatic ceramide content. Data are the mean ± SEM of n = 7-8 samples in each group.

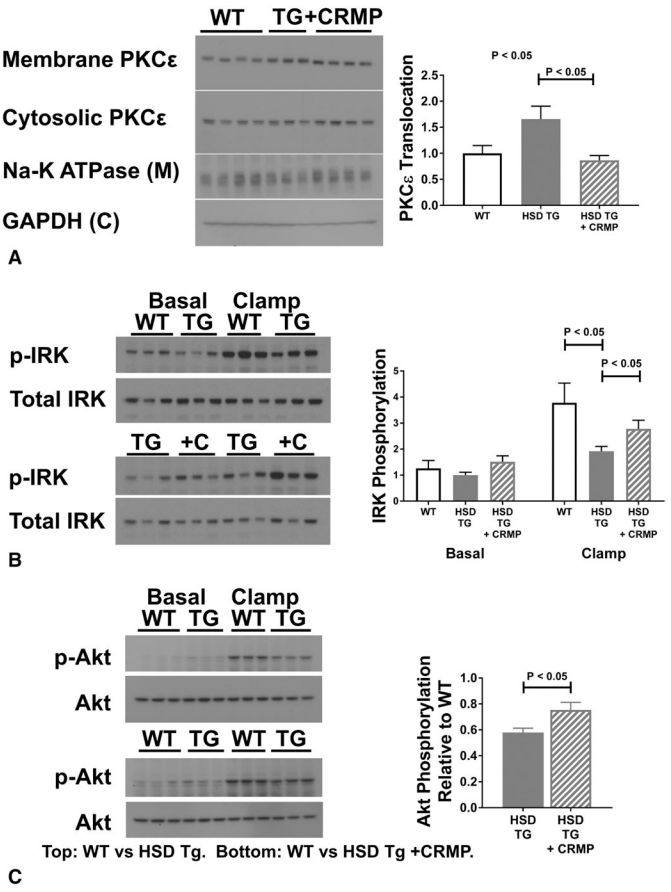

Figure 3. Hepatic insulin action.

A. Hepatic PKCε activation in six hour fasted livers, assessed by PKCε translocation. **B.** Hepatic insulin receptor kinase (IRK) tyrosine phosphorylation in the basal and clamped states. Blots on left compare WT livers with HSD Tg livers. Blots on right compare HSD Tg livers with HSD Tg + CRMP livers. For clarity, graphical representation includes data from both sets of immunoblots (normalized to untreated transgenic samples- the samples run on both sets of blots); for statistical analysis, only quantitation from within the same immunoblots was used. **C.** Hepatic insulin-stimulated Akt phosphorylation. Blots on top compare WT with HSD Tg; blots on bottom compare WT with HSD Tg + CRMP. Bar graph represents stimulation of Akt (phosphorylated Akt vs. total Akt), normalized to WT. Densitometry of individual groups presented in Supplemental Figure 2. Data are the mean ± SEM of n = 7 in each group (**A**); n = 6 in each group (**B-C**).

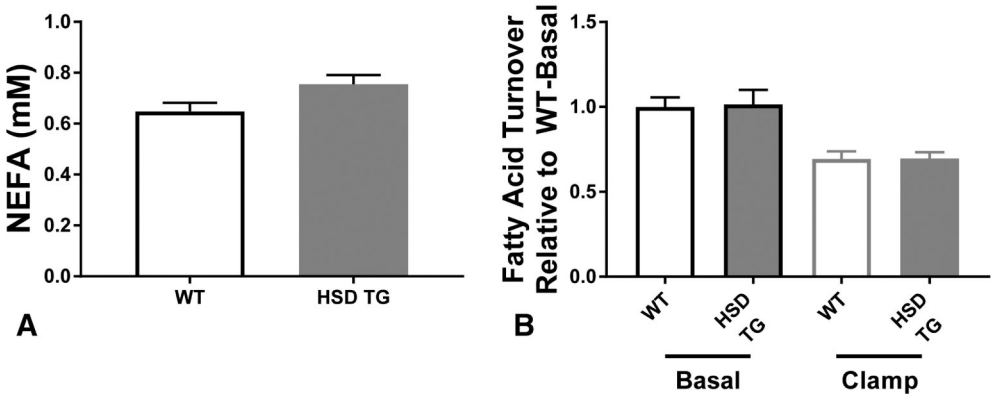

Figure 4. Plasma fatty acid parameters.

Plasma fatty acids, indices of adipose lipolysis, studied in WT and HSD Tg mice. **A.** Clamped plasma nonesterified fatty acid concentrations. **B.** Basal and clamped fatty acid turnover, expressed relative to basal fatty acid turnover. Data are the mean ± SEM of n = 7-8 samples in each group (**A**), and n = 10-18 in each group (**B**).

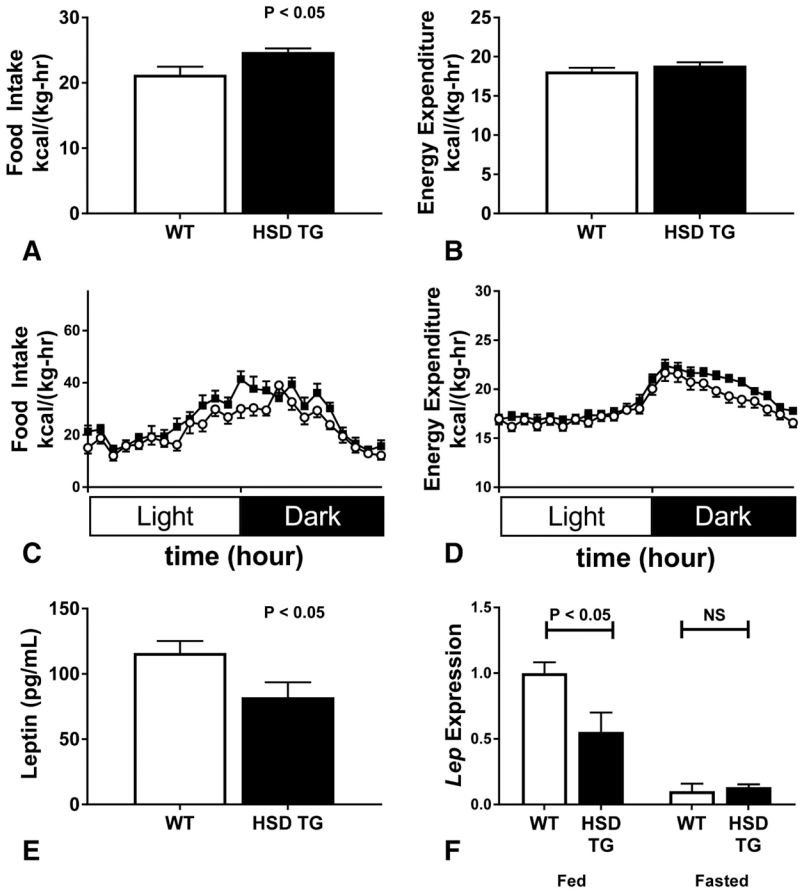

Figure 5. Plasma leptin levels and assessment of energy balance in metabolic cages.

A. Food intake in metabolic cages, normalized to total body mass, averaged over the course of the study period. **B.** Energy expenditure in metabolic cages, normalized to total body mass, averaged over the course of the study period. **C.** Hourly food intake, normalized to total body mass, averaged over the study period. WT- open circles; HSD transgenic- closed squares. **D.** Hourly energy expenditure, normalized to total body mass, averaged over the course of the study period. WT- open circles; HSD transgenic- closed squares. **E.** Fed-state early-morning plasma leptin levels. **F.** Adipose leptin gene expression in fed (left) or fasted (right) states. Data are the mean ± SEM of 12-14 animals in each group (**A-D**); n = 4-6 samples in each group (**E-F**).

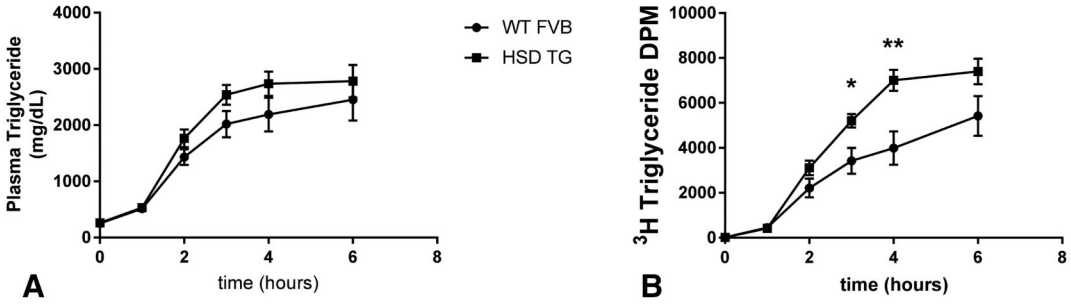

Figure 6. Oral fat tolerance tests.

Gavage of vegetable oil labeled with ^{3}H-Triolein at time = 0. **A.** Plasma triglycerides vs. time. **B.** Plasma chylomicrons reflected by ^{3}H-Triolein counts vs. time, represented as DPM in 5 μL plasma. Data are the mean ± SEM of n = 14 per group (**A**), n = 9-10 per group (**B**). * $P < 0.05$; ** $P < 0.01$.

Table 1:
Basal Body weights and Serum Chemistries.

Six hour fasted parameters.

	WT	HSD Tg	WT + CRMP	HSD Tg + CRMP
	n=8	n=7	n=7	n=8
Body Weight (g)	29.3 ± 0.9	29.6 ± 1.0	30.1 ± 1.0	30.1 ± 1.2
Epidydimal WAT Weight (g)	1.06 ± 0.12	1.06 ± 0.12	1.19 ± 0.10	1.07 ± 0.12
Insulin (μU/mL)	13 ± 4	17 ± 4	22 ± 4	19 ± 4
Plasma Triglyceride (mg/dL)	91 ± 12	79 ± 12	128 ±16	115 ± 8
NEFA (mM)	0.48 ± 0.02	0.43 ± 0.03	0.62 ± 0.07	0.51 ± 0.04
Glucose (mg/dL)	257 ± 9	281 ± 24	250 ± 20	256 ± 23